



Highly Hg²⁺-sensitive and selective fluorescent sensors in aqueous solution and sensors-encapsulated polymeric membrane

Journal:	<i>RSC Advances</i>
Manuscript ID	RA-ART-11-2015-022977.R1
Article Type:	Paper
Date Submitted by the Author:	05-Jan-2016
Complete List of Authors:	Kraithong, Sasiwimon ; Silpakorn University, Department of Chemistry Kittidachachan, Pattareeya ; Faculty of Science, King Mongkut's Institute of Technology Ladkrabang, Department of Physics Suwatpipat, Kullatat ; Silpakorn University - Sanam Chandra Palace Campus, Department of Chemistry, Faculty of Science Sirirak, Jitnapa; Silpakorn University - Sanam Chandra Palace Campus, Department of Chemistry, Faculty of Science Swanglap, Pattanawit; Silpakorn University, Department of Chemistry Wanichacheva, Nantanit; Silpakorn University, Department of Chemistry
Subject area & keyword:	Sensors < Analytical

Highly Hg²⁺-sensitive and selective fluorescent sensors in aqueous solution and sensors-encapsulated polymeric membrane

Sasiwimon Kraithong¹, Pattareeya Kittidachachan², Kullatat Suwatpipat¹, Jitnapa Sirirak¹,
Pattanawit Swanglap¹, Nantanit Wanichacheva^{1,*}

¹Department of Chemistry, Faculty of Science, Silpakorn University, Nakorn Pathom 73000, Thailand

²Department of Physics, Faculty of Science, King Mongkut's Institute of Technology Ladkrabang, Bangkok 10520, Thailand

*Corresponding Author : nantanit@su.ac.th, wanichacheva.nantanit@gmail.com

Abstract

Two Hg²⁺ chemosensors, rhodamine B hydrazide (**RBH**) and rhodamine 6G hydrazide (**R6GH**), were synthesized by a single step. In the presence of Hg²⁺, both of sensors **RBH** and **R6GH** exhibited highly sensitive OFF-ON fluorescence enhancement. Importantly, the sensors showed a selective binding to Hg²⁺ over other common metal ions such as K⁺, Na⁺, Fe³⁺, Ca²⁺, Cu²⁺, Ag⁺ and Pb²⁺ in aqueous solutions. The OFF-ON fluorescence enhancement upon Hg²⁺ binding could be ascribed to conformational change of spirolactam moiety of rhodamine fluorophore through spirolactam ring opening process. Furthermore, encapsulation of the sensors by polymeric membranes (PMMA) provided high selectivity and high sensitivity. Especially, sensors-encapsulated polymeric membrane **RBH** that showed extremely low detection limit (0.2 ppb), which was 245 times lower than sensor **RBH** in aqueous solution. In addition to fluorescence enhancement, the presence of Hg²⁺ also induced a noticeably color change from colorless to pink for the sensors dissolving in aqueous solution (10% v/v MeOH/water). The detection limits of sensor **RBH** and **R6GH** in both formats were in the range of 10⁻⁹ – 10⁻⁷ M of Hg²⁺ and were sufficient for on-site Hg²⁺ detection in the environmental and biological systems such as ground water, drinking water and edible fish. In particular, the extremely high sensitivity of the novel sensors-encapsulated polymeric membranes **RBH** could pave the way for development of real time Hg²⁺ detection portable device.

Keywords

rhodamine; Hg²⁺ chemosensor; polymeric membranes; encapsulated sensor

Introduction

Hg²⁺ and its derivatives are highly toxic pollutants^{1, 2} which are danger to human and other living species upon exposure. Contamination of Hg²⁺ in an environment can originate from various industrial sources such as oil drilling, power plant and steel plant. Inorganic mercury can be transformed to methyl mercury by bacteria, and can easily enter human body via the food chain.³⁻⁷ The accumulation of Hg²⁺ in human can lead to serious health problems such as damaging and dysfunction of brain, kidney, DNA and central nervous system.^{8, 9} Hg²⁺ in an environment are generally detected by traditional analytical methods, such as inductively coupled plasma mass spectrometry and atomic absorption/emission spectroscopy.¹⁰⁻¹¹ These method are expensive, time-consuming and requires sophisticated instrumentation which are not suitable for on-site detection of Hg²⁺. Therefore, cheaper, reliable and more practical methods for on-site Hg²⁺ detection are desirable. In particular, fluorescence-based sensors for Hg²⁺ detection have gained a lot of interests because the sensors require low cost, simple instrumentation, and provide low detection limit with adequate sensitivity and high selectivity.¹²⁻¹⁴

These Hg²⁺ fluorescence-based sensors were synthesized based on the fluorescence-active molecules, which included naphthalimide,¹⁵⁻¹⁹ dansyl,²⁰⁻²³ pyrene²⁴⁻²⁷ and fluorescein.²⁸⁻²⁹ Among these Hg²⁺ sensors, it have been reported that rhodamine-based sensors could worked effectively as “OFF-ON” Hg²⁺ fluorescent chemosensors via chelation-enhanced fluorescence (CHEF) mechanism. The rhodamine-based sensors exhibited excellent photophysical properties including absorption and

emission in visible wavelength, high sensitivity and high selectivity. Additionally, in the presence of Hg^{2+} a color change of the sensors can be visualized by naked-eye which resulted from selective ring opening of spirolactam in rhodamine molecules upon binding of Hg^{2+} .³⁰⁻⁴¹

The aim of our work is to design the fluorescence-based sensors which can provide high sensitivity and selectivity for Hg^{2+} detection. The sensors should be produced by inexpensive starting materials, through a simplistic synthetic route and the sensors should be able to further develop to use for an on-site Hg^{2+} detection. With all these criteria in mind, we have prepared two types of sensors based on rhodamine derivatives to serve as fluorescence-active molecules. These two rhodamine derivatives were based on a hydrazine molecule which was covalently bound to rhodamine B moiety (**RBH**) and rhodamine 6G moieties (**R6GH**) as shown in Fig. 1. Sensor **RBH** has been reported for Hg^{2+} -sensing⁴¹ but **R6GH** molecule have not been previously tested as Hg^{2+} sensor. In this study, we sought to increase the sensitivity of the fluorescence-based Hg^{2+} sensor by employing **R6GH** as the fluorophore instead of **RBH** because **R6GH** provides larger molar extinction coefficients as well as higher quantum yield.⁴²⁻⁴³ Therefore, we expected enhancement in sensitivity of the designed sensor by using of **R6GH** as the fluorophore which is necessary for the development of economical portable Hg^{2+} -sensing devices.

These bare (Hg^{2+} free) rhodamine-based sensors were in spirolactam conformations, which were colorless and non-fluorescent. The addition of Hg^{2+} led to spirolactam ring opening via coordination or irreversible chemical reaction,^{32, 33} resulting in the appearance of a pink color (“OFF-ON” fluorescence switch). The colorimetric change and “turn-on” fluorescence behavior of sensors upon Hg^{2+} chelating observed here could potentially be used in portable devices and test kit for “naked-eye” Hg^{2+} detections.^{15, 37-39, 44-47} In addition, encapsulation of the other fluorescence sensors have been previously reported, the encapsulation led to more convenient use of the sensors, which still exhibited high sensitivity while maintaining high selectivity.⁴⁸⁻⁵¹ In this work, we also sought to increase the sensitivity and ease of use of our Hg^{2+} sensors therefore we tried encapsulating our sensors with PMMA onto glass slides. We found that both of our sensors in solution and the encapsulated ones were extremely selective to Hg^{2+} binding with negligible interferences from other metal ions. All of the sensors also provided high sensitivity with Hg^{2+} detection limits at concentration of ppb level.

Particularly, sensors-encapsulated polymeric membranes **RBH** exhibited very low detection limit (0.2 ppb) that was roughly 245 times lower than sensor **RBH** in solution. The extremely high sensitivity of the sensors-encapsulated polymeric membranes **RBH** could pave the way for development of real time Hg^{2+} detection portable device.

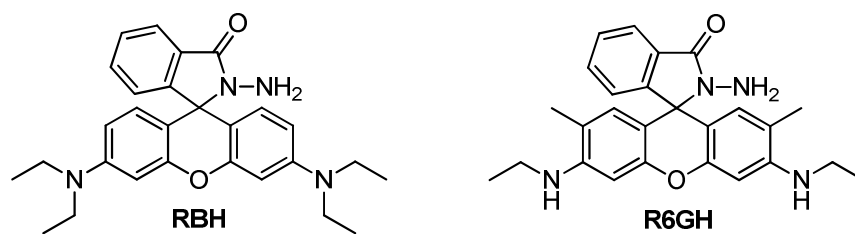


Fig. 1 Structures of sensor **RBH** and **R6GH**.

Experimental

Materials

All reagents and solvents were purchased from Fluka Chemical Corporation and were used as received. All of the metal salts used in this study were acetate salts and were purchased from Strem chemicals, Inc.

Methods

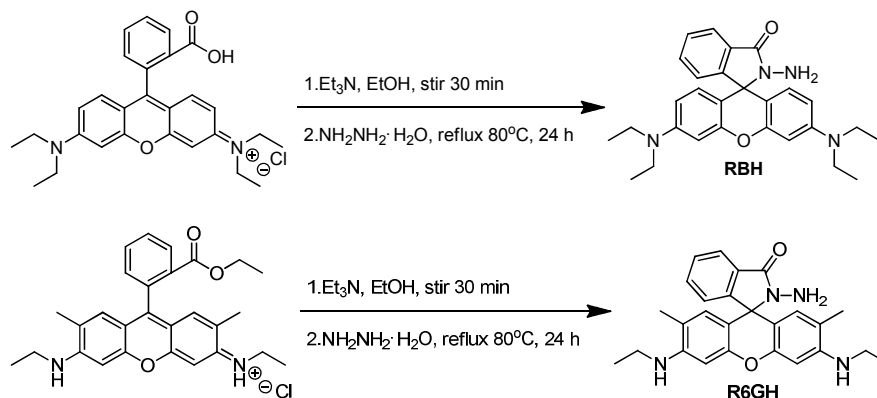
NMR spectra were obtained by a Bruker Avance 300 spectrometer operating at 300 MHz for ^1H and 75 MHz for ^{13}C . All NMR spectra were obtained in CDCl_3 solutions with TMS as the internal standard. Melting point was carried out by Stuart Scientific melting point apparatus SMP2. Mass spectra were performed by a ThermoElectron LCQDECA-XP, electrospray ionization ion trap mass spectrometer. Absorption spectra were determined by a single beam Hewlett Packard 8453 spectrophotometer. Fluorescence measurements were performed on a Perkin Elmer Luminescence spectrometer LS 50B. The excitation and emission slit widths were 5.0 nm. Fabrications of the sensors-encapsulated polymeric membranes were performed by a spin coater operated at 5000 rpm for 40 seconds. Computational experiments and DFT calculations were carried out using Gaussian 09 program⁵² and the geometry optimization at the DFT-B3LYP level using 6-311G** for main group element and LanL2DZ.⁵²⁻⁵³ The optimized structure of **RBH**, **R6GH**, **RBH:Hg²⁺** complex and **R6GH:Hg²⁺** complex were generated by VMD.⁵⁴

Synthesis of rhodamine B hydrazone (RBH)

The synthesis of the sensor **RBH** was obtained in the same manner as described previously³⁶ and the synthetic steps are outlined in Scheme 1. ^1H NMR (300 MHz, CDCl_3): δ 1.12 (t, 12H, $J = 6.9$ Hz), 3.29 (q, 8H, $J = 6.6$ Hz), 3.62 (br-s, 2H, NH_2), 6.24 (dd, 2H, $J_1 = 8.7$ Hz, $J_2 = 2.4$ Hz), 6.40-6.43 (m, 4H), 7.01 (dd, 1H, $J_1 = 5.4$ Hz, $J_2 = 3.0$ Hz), 7.34-7.37 (m, 2H), 7.91 (dd, 1H, $J_1 = 5.7$ Hz, $J_2 = 3.0$ Hz) ppm; ^{13}C NMR (75 MHz, CDCl_3): δ 12.54 (4 CH_3), 44.25 (4 CH_2), 65.58 (C), 98.02 (2CH), 104.71 (2C), 107.97 (2CH), 122.73 (CH), 123.68 (CH), 127.88 (CH), 127.97 (2CH), 129.93 (2C), 132.36 (CH), 148.71 (2C), 151.56 (C), 153.8 (C), 165.88 (C) ppm.

Synthesis of rhodamine 6G hydrazone (R6GH)

The synthesis procedure of **R6GH** was modified from the previous study.⁴¹ In a 10 mL round bottom flask, a mixture of rhodamine 6G (0.10 g, 0.21 mmol) and triethylamine (0.10 mL, 1.7 mmol) in ethanol (5 mL) was stirred for 30 min under an argon atmosphere. Then, hydrazine monohydrate (0.10 mL, 2.0 mmol) was added in to the mixture. After that, the solution was refluxed for 24 h under argon atmosphere (the precipitation could be observed soon after the mixture was heated). After cooling to room temperature, the precipitation was filtered and dried to give pale pink powder 67 mg, 75% yield, m. p. 263-265 °C; ^1H NMR (300 MHz, CDCl_3): δ 1.32 (t, 6H, $J = 7.2$ Hz), 1.92 (s, 6H), 3.21-3.23 (m, 4H), 3.52 (br-s, 1H, NH), 3.59 (br-s, 2H, NH_2), 6.26 (s, 2H), 6.39(s, 2H), 7.05-7.08 (m, 1H), 7.42-7.48 (m, 2H), 7.94-7.99 (m, 1H) ppm; ^{13}C NMR (75 MHz, CDCl_3): δ 14.77 (2 CH_3), 16.71 (2 CH_3), 38.37 (2 CH_2), 66.06 (C), 96.84 (2CH), 104.92 (2C), 117.99 (2C), 123.04 (CH), 123.81 (CH), 127.70 (2CH), 128.13 (CH), 129.86 (C), 132.59 (CH), 141.54 (2C), 151.75 (C), 152.24 (2C), 166.22 (C) ppm; HR-ESI MS calcd for $\text{C}_{26}\text{H}_{28}\text{N}_4\text{NaO}_2^+$ ($\text{M}+\text{Na}$)⁺ 451.2104 m/z, found 451.2112 m/z.



Scheme 1 Synthesis of **RBH** and **R6GH**

Preparation of sensors-encapsulated polymeric membranes

The single layer luminescent films were prepared by spin coating the fluorescent sensor **RBH** or **R6GH** mixed in polymer solution onto microscope glass slides. First, the solutions of sensors **RBH** and **R6GH** were prepared by dissolving 0.0081 g of sensor **RBH** or 0.0109 g of sensor **R6GH** in 10 ml of chloroform (AR grade). Then, 0.30 g of PMMA was added to the sensor solutions and the mixtures were sonicated for 20 minutes. The mixtures were then poured onto the substrate and spin coated at constant speed of 5000 rpm for 40 seconds and were left to dry at room temperature for 1 day.

Hg²⁺ binding affinity and sensitivity studies

The binding studies of sensors **RBH** and **R6GH** were carried out in MeOH for UV-visible study and in 10% v/v MeOH/water for fluorescence measurement. The acetate salts solutions (1.0×10^{-2} M) were prepared by dissolving the desired amount of acetate salts in deionized water. The fluorescence titration was performed by measuring fluorescence intensities of solutions of **RBH** and **R6GH** (4.4×10^{-6} M) as a function of concentrations of added metal ions over a fixed wavelength range (500 – 650 nm). The excitation wavelength was (λ_{ex}) 500 nm for sensors **RBH** and **R6GH**. The sensitivity of sensors **RBH** and **R6GH** encapsulated polymeric membranes were tested by immersion of the membranes in 10% v/v MeOH/water solutions with different Hg²⁺ concentrations.

Result and discussion

Molecular design and synthesis of **RBH** and **R6GH**

Sensors **RBH** and **R6GH** were synthesized according to the synthetic outlined in **Scheme 1**. Rhodamine B hydrazide (**RBH**) and rhodamine 6G hydrazide (**R6GH**) were prepared by amidation reaction of rhodamine B or rhodamine 6G hydrochloride with hydrazine monohydrate.^{36, 41} The synthetic route was simple, used only one-step synthesis and required inexpensive starting materials. The sensors structures were confirmed by ESI data, ¹H NMR and ¹³C NMR spectra as shown in section 2.

The characterizations confirmed that the structure consisted of two nitrogen atoms at the chelating sites, which were covalently bound to rhodamine B and rhodamine 6G subunits. Based on the spiro lactam (non-fluorescent) to ring-opening spiro lactam (fluorescent) equilibrium of rhodamine, the sensor structures were designed by considering the electrostatic-structural change. Consequently, the chelation between the carbonyl oxygen and nitrogen atoms of the sensors and Hg²⁺ could occur via favorable electrostatic interactions, resulting in both fluorescence enhancement and a colorimetric change. In addition to utilizing of the sensors in solutions, the polymeric membranes of both sensors-encapsulated by PMMA coated on glass slides were also prepared for portable test kit application.

Sensitivity studies in aqueous solutions

The sensitivity study of sensor **RBH** for determination of Hg²⁺ has been reported by Kim and coworkers.⁴¹ The maximum absorption of sensor **RBH** dissolving in MeOH was 550 nm. In our work, we also tested Hg²⁺ detection of sensor **RBH** in 10% v/v MeOH:water. In the presence of Hg²⁺, the fluorescence emission of sensor **RBH** was strongly enhanced at 573 nm and was accompanied by chromogenic changes of the sensor (from colorless to pink). The detection limits were calculated from the plot of the fluorescence intensities as a function of the Hg²⁺ concentrations as describe in the previous study⁵⁵ and the detection limit of sensor **RBH** in solution was 2.4×10^{-7} M or 49 ppb and the association constant, K_{assoc} , of sensor **RBH** was 4.65×10^7 M⁻¹.

In contrast, **R6GH** sensor has never been reported as a sensitive and selective Hg²⁺-sensor. The maximum absorption of sensor **R6GH** in MeOH was 525 nm as shown in Fig. 2a. In the absence of Hg²⁺, the solution of sensor **R6GH** was colorless and did not exhibit fluorescence. Upon gradual titration of Hg²⁺, strong absorption band at approximately 525 nm was observed as well as the color of the solution was changed from colorless to pink which could be seen by bare eyes.

A narrow peak (shoulder) at approximately 480 nm in the absorbance spectra of sensor **R6GH** (Fig. 2) could be ascribed to the change of photophysical properties of the absorption due to the acidity environment caused by solvent and addition of Hg^{2+} . In this work, solvent (MeOH) is slightly acidic and could lead to an appearance of the shoulder in the absorption spectra. This change of an absorption due to ionization of the fluorescence molecule caused by change of pH could be observed in the fluorescence molecule, and has been well explained and demonstrated.⁵⁶ In addition, it has been previously reported that adding of Hg^{2+} in to rhodamine-based fluorescence molecule could lead to appearance of the shoulder in the absorption spectra due to Hg^{2+} -induced spirolactam ring-opening, which resulted in change of photophysical properties of the absorption.⁵⁷

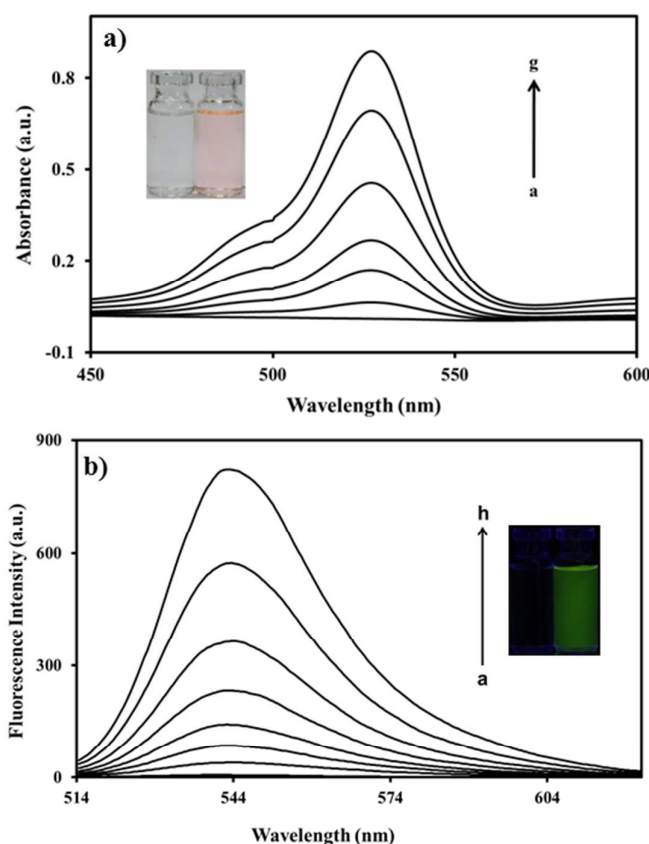


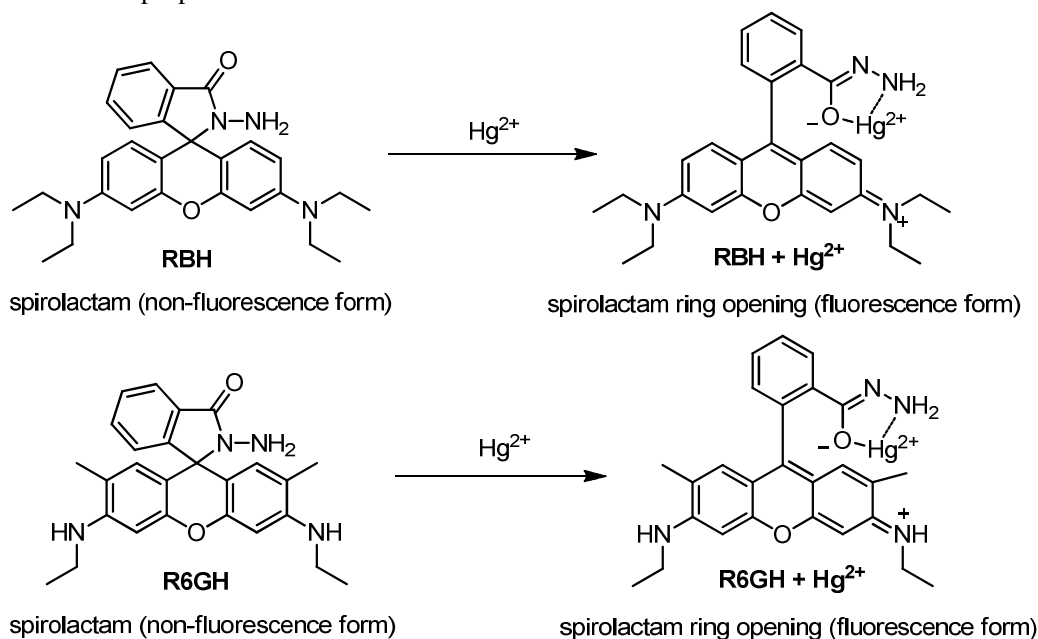
Fig. 2 a) UV-Visible absorption spectra of sensor **R6GH** ($0.33 \mu\text{M}$) in MeOH with addition of $[\text{Hg}^{2+}]$ a: $0 \mu\text{M}$, b: $7.2 \mu\text{M}$, c: $29 \mu\text{M}$, d: $36 \mu\text{M}$, e: $43 \mu\text{M}$, f: $50 \mu\text{M}$, g: $56 \mu\text{M}$. b) Fluorescence titrations ($\lambda_{\text{ex}} = 500 \text{ nm}$) of sensor **R6GH** ($4.4 \mu\text{M}$) in 10% v/v MeOH/water with addition of $[\text{Hg}^{2+}]$ a: $0 \mu\text{M}$, b: $4.4 \mu\text{M}$, c: $10 \mu\text{M}$, d: $14 \mu\text{M}$, e: $19 \mu\text{M}$, f: $26 \mu\text{M}$, g: $35 \mu\text{M}$, h: $44 \mu\text{M}$.

The quantitative analysis of sensors **R6GH** was carried out by monitoring the rhodamine fluorescence with excitation wavelength at 500 nm. The fluorescence intensity changes of the sensor were monitored upon the addition of metal ions to determine the cations binding capacities. Fig. 2b shows the emission spectra of sensor **R6GH** in the presence of different concentrations of Hg^{2+} , respectively. The fluorescence behaviors of sensor **R6GH** clearly demonstrated the “OFF-ON” switching mechanism. In the absence of Hg^{2+} , the solution of the sensor provides weak emission signals (non-fluorescence). Whereas the addition of Hg^{2+} resulted in the fluorescence “turn-on”, with the intensities of the emitted fluorescence increased as a function of Hg^{2+} concentration. The fluorescence emission was consequence of rapidly enhanced strong emissions at 540 nm. Furthermore, sensor **R6GH** also exhibited chromogenic changes (colorless to pink).

As we expected, the detection limit of sensor **R6GH** in solution was improved to 2.9×10^{-8} M or 5.9 ppb compared to rhodamine B hydrazide system (49 ppb). It should be noted that in solutions, the sensitivity of sensor **R6GH** employing rhodamine 6G has improved significantly compared to the sensor that employing **RBH** (detection limits are 5.9 ppb and 49 ppb, respectively). This enhancement in sensitivity is possibly due to a higher emission quantum yield of rhodamine 6G ($\Phi_f = 0.94$ in EtOH)⁴² compared to that of rhodamine B ($\Phi_f = 0.69$ in EtOH).⁴³ The sub-micromolar detection limit of our sensor is sufficient for Hg^{2+} ions detection in the environmental and many biological systems such as ground water, drinking water and edible fish. The association constant, K_{assoc} , observed from the changes of intensities in the fluorescence titration, of sensor **R6GH** was $7.13 \times 10^9 \text{ M}^{-1}$ and 1:1 complex formation of sensor **R6GH** with Hg^{2+} was suggested. The K_{assoc} was determined utilizing the Benesi–Hildebrand plot as described in previous studies.⁵⁸⁻⁵⁹

Binding mechanism of the sensors

The photophysical properties, NMR data and molecular modeling results illustrated that the binding of the sensors and Hg^{2+} ions took place through electrostatic interactions between the carbonyl oxygen and nitrogen atoms of the sensors and Hg^{2+} . The selective binding resulted in change of the structures from the spirolactams (non-fluorescent forms) of **RBH** and **R6GH** to the non-cyclic forms (fluorescent forms) as indicated by the OFF-ON fluorescence signal upon Hg^{2+} binding. The operation of the sensors are proposed and shown in Scheme 2.



Scheme 2 Proposed operation of sensors **RBH** and **R6GH**: before binding to Hg^{2+} (left) and after binding to Hg^{2+} (right)

The large fluorescence enhancement of **RBH** (at 573 nm) and **R6GH** (at 540 nm) could be corresponded to ring opening spirolactam conformation of the rhodamine units, which was induced by the complexation of Hg^{2+} ions. When the sensors coordinated with the Hg^{2+} ions, the rhodamine structure contained more conjugated double bonds from the opening form of the spirolactam ring which resulted in an increase of the fluorescence intensity.

^{13}C -NMR titration results clearly supported the proposed ring-opening mechanism. As demonstrated in Fig. 3, the chemical shift of the quaternary carbon of **RBH** at 65.6 ppm^{60} was disappeared indicating a spirocycle ring opening upon the addition of Hg^{2+} . In addition, the appearance of new signal at 175.6 ppm , which corresponded to carbonyl carbon of amide functional group⁶¹, indicated spirocycle ring opening and the amide formation.

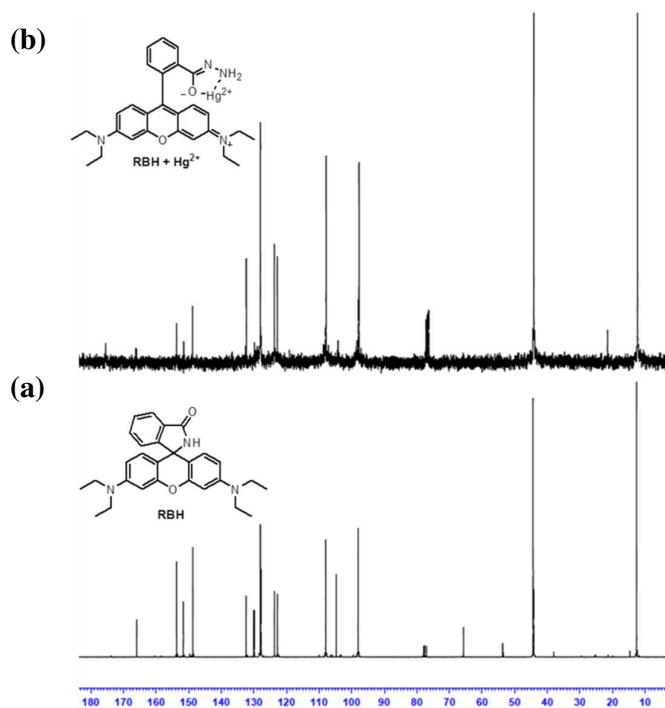


Fig. 3 ^{13}C -NMR spectra of **RBH** in the absence of Hg^{2+} (a) and in the presence of Hg^{2+} (b)

A similar behavior was observed for **R6GH**, the addition of Hg^{2+} led to lower intensity of the quaternary carbon at 66.1 ppm^{60} as well as the appearance of new signal of carbonyl carbon of amide at 175.9 ppm^{61} , indicated that Hg^{2+} induced spirocycle ring opening (Fig 4.).

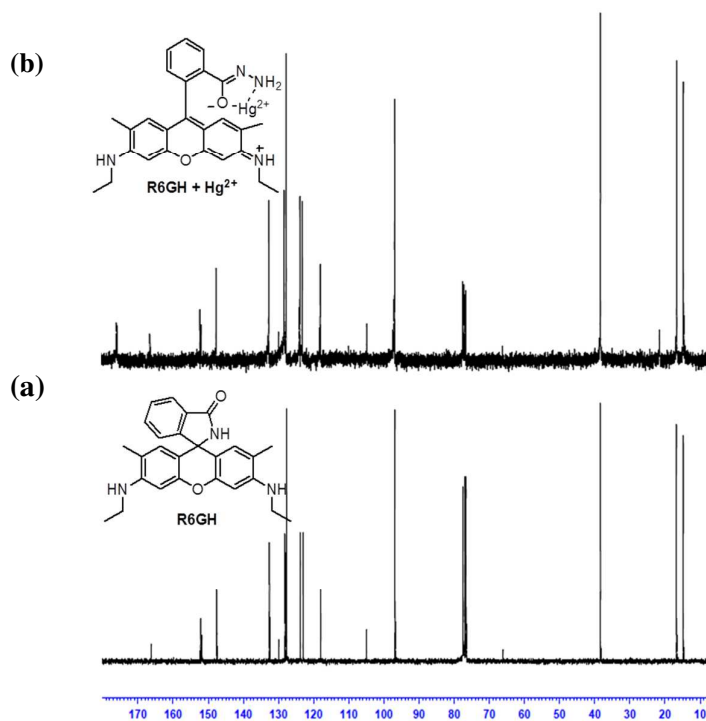
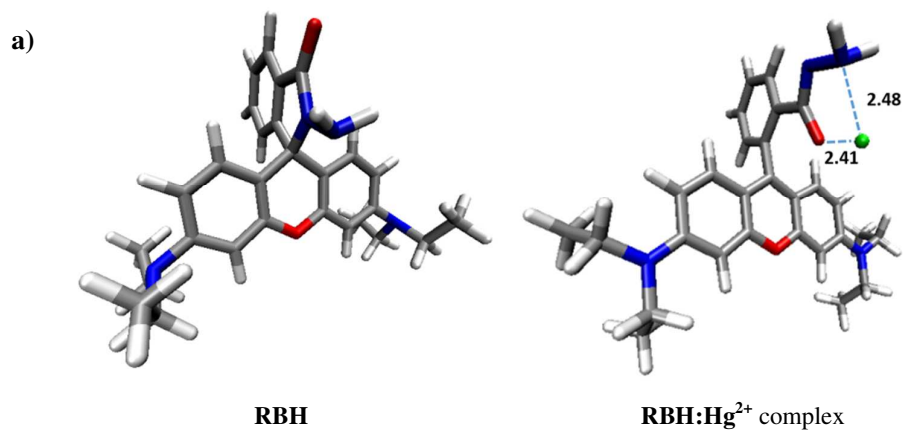


Fig. 4 ^{13}C -NMR spectra of **R6GH** in the absence of Hg^{2+} (a) and in the presence of Hg^{2+} (b)

In order to clarify the coordination geometry of **RBH** and **R6GH** and investigate the Hg^{2+} binding to **RBH** and **R6GH**, Gaussian 09⁵² was employed to perform the geometry optimization at the DFT-B3LYP level using 6-311G** for main group element and LanL2DZ⁵²⁻⁵³ for Hg^{2+} in 10% v/v MeOH:water with the integral equation formalism polarizable continuum model (IEEPCM). The optimized structure of **RBH**, **R6GH**, **RBH**· Hg^{2+} complex and **R6GH**· Hg^{2+} complex generated by VMD⁵⁴ were shown in Fig. 5.



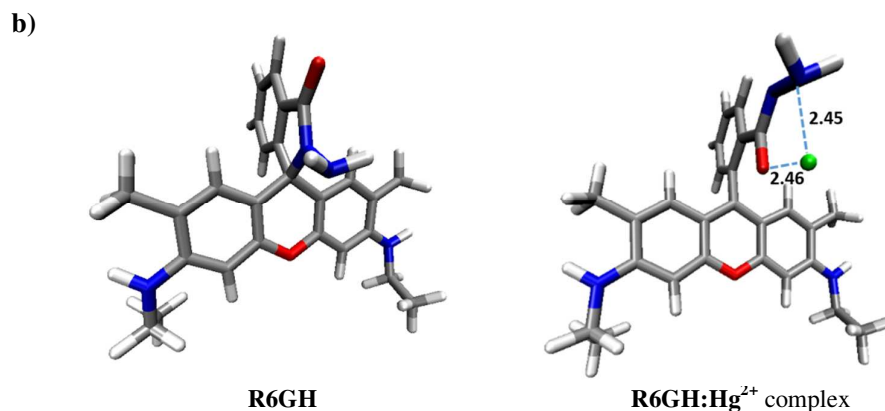


Fig. 5 a) Optimized structure of **RBH** and **RBH:Hg²⁺** complex b) Optimized structure of **R6GH** and **R6GH:Hg²⁺** complex obtained at the B3LYP level using 6-311G** for main group element and LanL2DZ for Hg²⁺ in 10% v/v MeOH:water with the integral equation formalism polarizable continuum model (IEEPCM).

The optimized structures of the host-guest complexes in 10% v/v MeOH:water are shown in Fig. 5. The optimized structures revealed that ions-recognition of both sensors were originated from the favorable electrostatic interactions (via electrostatic interactions and cation-dipole interactions) of the carbonyl oxygen atom (from rhodamine portion) and nitrogen atom (from hydrazine portion) with Hg²⁺ ion. The distances that indicate the binding sites of Hg²⁺ bound to **RBH** and **R6GH** are illustrated in Fig. 5 (a and b). From the optimization using DFT, for **RBH:Hg²⁺** complex, Hg²⁺ was coordinated by the carbonyl oxygen and nitrogen atoms with the distances of 2.41 Å and 2.48 Å while for **R6GH:Hg²⁺** complex, Hg²⁺ was bound to the carbonyl oxygen and nitrogen atoms with the distances of 2.46 Å and 2.45 Å, respectively.

Selectivity studies in aqueous solutions

The fluorescence emission of sensor **R6GH** in the presence of various transition metal ions was investigated in 10% v/v MeOH/water to evaluate their potential utilization as a fluorescent sensor for cations recognition. The selectivity of the sensor was studied by the method which was similar to the separate solution method (SSM) that was used in ion-selective electrode applications.⁶² The SSM method measures a series of separate solutions with each solution bearing only a salt of the determined ion. The selectivity of fluorescent sensor **R6GH** have been carried out by recording the fluorescence intensities of the sensor as a function of concentrations of different metal cations including Ag⁺, Ca²⁺, Cu²⁺, K⁺, Na⁺, Pb²⁺ and Fe³⁺.

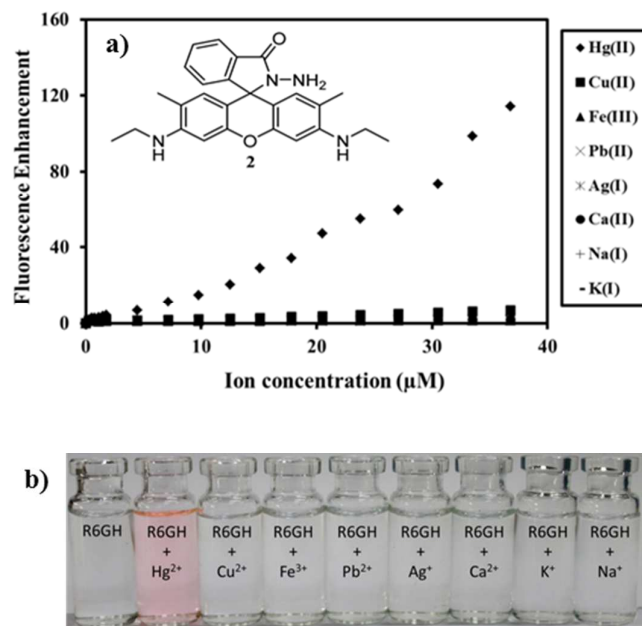


Fig. 6 a) Fluorescence enhancement (540 nm) of **R6GH** (4.4 μM) as a function of the concentrations of various metal ions in 10% v/v MeOH/water. b) Color changes of sensor **R6GH** (4.4 μM) in the absence and presence of Hg²⁺, Ag⁺, Ca²⁺, Cu²⁺, K⁺, Na⁺, Pb²⁺ and Fe³⁺ (λ_{ex} = 500 nm).

Selectivity study revealed that sensor **R6GH** exhibited much stronger binding affinity to Hg²⁺ than other metal ions as illustrated in Fig. 6a. It can be seen that only Hg²⁺ led to a significant increase of fluorescence intensity (fluorescence enhancement), while addition of other metal cations such as Ag⁺, Ca²⁺, Cu²⁺, K⁺, Na⁺, Pb²⁺ and Fe³⁺ barely affected the fluorescence intensities. The selectivity results suggested that sensor **R6GH** was a Hg²⁺-selective fluorescent sensors in aqueous solution and Ag⁺, Cu²⁺ and Pb²⁺ which were potential competitors^{15, 63-67} could not interfere Hg²⁺ detection of the sensors. The high selectivity of sensor **R6GH** presented here was expected due to the favorable electrostatic interactions of Hg²⁺ to the sensors because of the appropriate charge and size of Hg²⁺ which promote the interaction of Hg²⁺ with N donor atom of the hydrazine ligand and the O donor atom of the rhodamine moiety, which occurred via the cation-dipole interaction and cation-anion interaction.^{34-36, 41}

The selective determination was not only indicated by fluorescence enhancement but also by a colorimetric change, as presented in Fig. 6b. Upon the addition of Hg²⁺ to the solution of **R6GH**, the color change of the solutions from colorless to pink could be easily observed by the bare eyes, while the titration of other ions (Ag⁺, Ca²⁺, Cu²⁺, K⁺, Na⁺, Pb²⁺ and Fe³⁺) with concentrations greater than 10 equivalents of Hg²⁺ induced no color changes in the solutions.

Studies of sensors-encapsulated polymeric membranes

Real time and on-site analysis application such as portable test kit utilizing our sensors is possible due to the excellent optical properties of the sensors such as strong absorption and fluorescence in visible wavelength in the presence of Hg²⁺. In this work we demonstrated portable test kit for Hg²⁺ detection by encapsulation fluorescent sensors **RBH** and **R6GH** in a low cost polymer (PMMA) and then coated the sensors onto glass slides to serve as portable sensors for Hg²⁺ determination.

The sensors-encapsulated polymeric membranes **RBH** and **R6GH** were immersed in 10% v/v MeOH/water containing different Hg²⁺ concentrations. The fluorescence intensities at 658 nm for **RBH** and at 665 nm for **R6GH** were then recorded as a function of Hg²⁺ concentrations as shown in Fig. 7a and 7b.

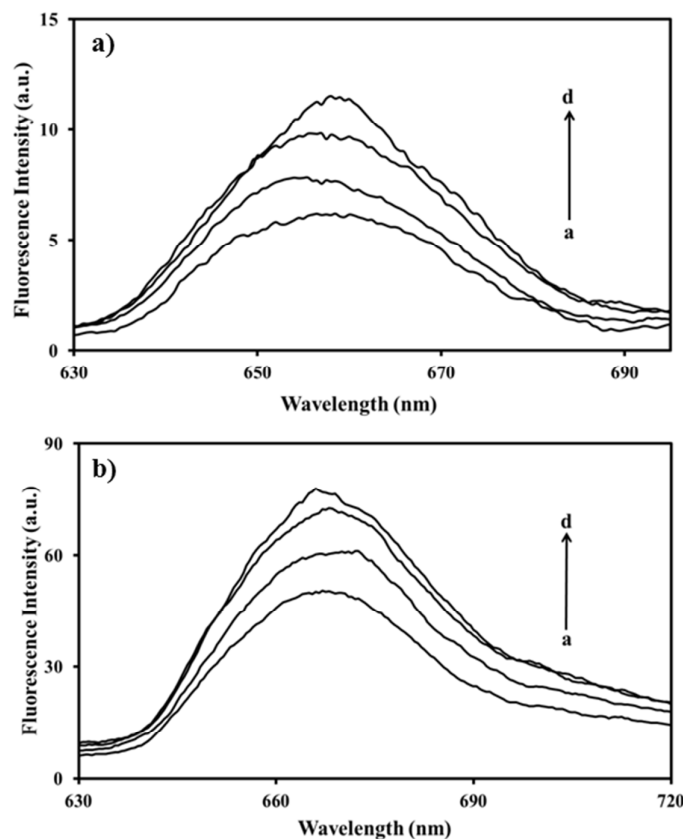
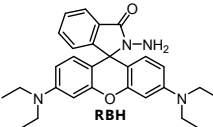
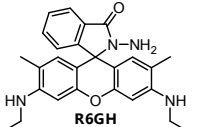


Fig. 7 a) Fluorescence titrations ($\lambda_{\text{ex}} = 500$ nm) of the polymeric membranes **RBH** in 10% v/v MeOH/water with addition of $[\text{Hg}^{2+}]$ a: 0 μM , b: 0.9 μM , c: 1.5 μM , d: 89 μM . b) Fluorescence titrations ($\lambda_{\text{ex}} = 500$ nm) of the polymeric membranes **R6GH** in 10% v/v MeOH/water with addition of $[\text{Hg}^{2+}]$ a: 0 μM , b: 0.1 μM , c: 1.9 μM , d: 3.3 μM .

The detection limits of the sensors-encapsulated polymeric membranes **RBH** and **R6GH** were 1.1×10^{-9} M or 0.2 ppb and 5.9×10^{-8} M or 12 ppb, respectively. The association constant, K_{assoc} , observed from the changes of intensities in the fluorescence titration, of sensors-encapsulated polymeric membranes **RBH** and **R6GH** were 1.13×10^7 M^{-1} and 6.26×10^8 M^{-1} , respectively. Table 1 illustrates the comparison of analytical parameters for sensors employing **RBH** and **R6GH** in solutions and polymeric membranes for determination of Hg^{2+} .

Table 1. Analytical parameters of sensors employing **RBH** and **R6GH** in solutions and PMMA membranes

Sensor	Working system	$\lambda_{\text{ex}}/\lambda_{\text{em}}$ (nm)	Detection limit	Working range
 RBH	MeOH/H ₂ O (1:9 v/v)	500/573	$2.4 \times 10^{-7} \pm 1.2 \times 10^{-8}$ M (49 \pm 2.3 ppb)	500-2500 ppb
	Polymer film	500/658	$1.1 \times 10^{-9} \pm 3.1 \times 10^{-10}$ M (0.2 \pm 0.063 ppb)	50-750 ppb
 R6GH	MeOH/H ₂ O (1:9 v/v)	500/540	$2.9 \times 10^{-8} \pm 6.2 \times 10^{-9}$ M (5.9 \pm 1.3 ppb)	100-250 ppb
	Polymer film	500/665	$5.9 \times 10^{-8} \pm 1.1 \times 10^{-8}$ M (12 \pm 2.2 ppb)	100-700 ppb

Remarkably, the encapsulated sensor **RBH** exhibited approximately 245 times lower detection limit than the detection limit of sensor **RBH** dissolving in the solution. The drastically low detection limit of the encapsulated sensor **RBH** could be attributed to both slower motion of Hg^{2+} and the proper orientation of the sensor, which promoted binding of Hg^{2+} , in confined spaces (pores) of PMMA film

Due to the extremely low detection limit of sensors-encapsulated polymeric membrane **RBH**, the further investigation on Hg^{2+} binding to **RBH** in environment which has similar dielectric constant (ϵ) to that of polymeric membranes (PMMA) ($\epsilon=3.6$)⁶⁸ was also performed. Using the optimized structure of **RBH:Hg²⁺** complex in 10% v/v MeOH:water as the starting structure, the **RBH:Hg²⁺** complex was optimized at the B3LYP level using 6-311G** for main group element and LanL2DZ for Hg^{2+} with the integral equation formalism polarizable continuum model (IEEPCM) and dielectric constant of 3.6.

As illustrated in Fig. 8, the optimized structure of **RBH:Hg²⁺** complex in PMMA showed that Hg^{2+} was bonded by carbonyl oxygen atom and nitrogen atom with shorter distances than those of **RBH:Hg²⁺** complex in 10% v/v MeOH:water (Fig 5a). The complexation energy of **RBH:Hg²⁺** complex in PMMA calculated from the Energy of complex – Energy of **RBH** – Energy of Hg^{2+} was equal to -63.23 kcal/mol, indicated a good stability of this complex in PMMA polymer film, which was 56 kcal/mol lower than that of **RBH:Hg²⁺** complex in 10% v/v MeOH:water.

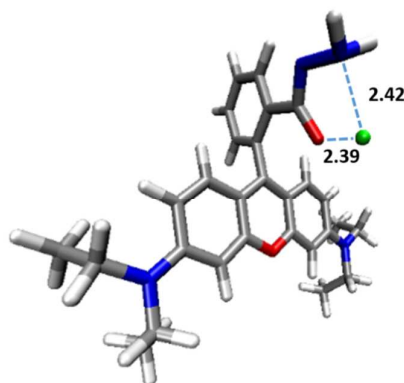


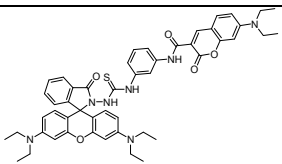
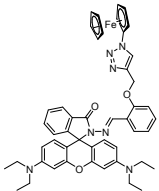
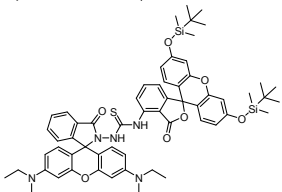
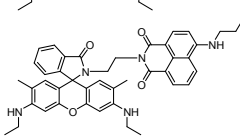
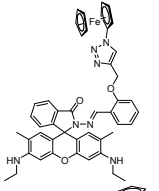
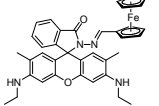
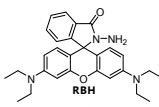
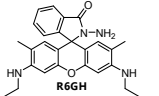
Fig. 8 Optimized structure of **RBH:Hg²⁺** complex obtained at the B3LYP level using 6-311G** for main group element and LanL2DZ for Hg^{2+} with the integral equation formalism polarizable continuum model (IEEPCM) and dielectric constant (ϵ) of 3.6.

The higher detection limit of **R6GH** than **RBH** in sensors-encapsulated polymeric membranes could be attributed to polarities of the sensors and PMMA film. Justifying from the chemical structure shown in Fig. 1, **RBH** is more hydrophobic than **R6GH**, therefore **RBH** should dissolve and disperse in PMMA much better than **R6GH** due to high hydrophobicity of PMMA. Therefore, the concentration of the incorporated **RBH** in PMMA film should be higher than **R6GH** which resulted in lower detection limit of **RBH** than **R6GH** in sensors-encapsulated polymeric membranes. The molecular modeling of **R6GH:Hg²⁺** complex in PMMA showed the difficulty to optimize, which indicated a less stability of this complex in PMMA polymer film compared to that of **RBH:Hg²⁺** complex, which could result in lower sensitivity and higher detection limit of **R6GH** compared to **RBH** in sensors-encapsulated polymeric membranes.

However, the colorimetric change upon addition of Hg^{2+} was not observed for the encapsulated sensors, which could be caused by the change in photophysic (absorption) of the sensors due to encapsulation of the sensors by PMMA. The detection limit of the encapsulated sensor **RBH** in PMMA film was 10 times lower than the allowed maximum concentration of Hg^{2+} in the environmental (2 ppb) of US EPA¹, and was lower than the recently reported rhodamine-based Hg^{2+} sensors⁶⁹⁻⁷³ as shown in Table 2. However, it should be noted that the detection limit of both

encapsulated sensors were sufficient for detection of Hg^{2+} in the environmental samples while providing convenience for using and transportation of the sensors.

Table 2. Comparison of the recently reported rhodamine sensors for determination of Hg^{2+}

Hg^{2+} -sensor	Working system	$\lambda_{\text{ex}}/\lambda_{\text{em}}$ (nm)	Enhancement (times)	Detection limit	References
	EtOH/HEPES buffer (pH 7.4, 50:50 v/v)	440/478, 587	18, 78	3.2×10^{-9} M (0.64 ppb)	69
	CH_3CN /HEPES buffer (pH 7.3, 2:8 v/v)	495/585	57	1.7×10^{-8} M (3.4 ppb)	70
	CH_3CN /Tris-HCl buffer (pH 7.4, 1:1 v/v)	480/592	26	5.4×10^{-9} M (1.1 ppb)	71
	CH_3CN	450/520, 550	15, 3	7.9×10^{-7} M (0.15 ppm)	72
	CH_3CN /HEPES buffer (pH 7.3, 2:8 v/v)	480/554	20	1.4×10^{-8} M (2.8 ppb)	70
	H_2O	500/550	48	5.0×10^{-9} M (1.0 ppb)	73
	Polymer film	500/658	2	1.1×10^{-9} M (0.2 ppb)	This work
	$\text{MeOH}/\text{H}_2\text{O}$ (1:9 v/v)	500/540	218	2.9×10^{-8} M (5.9 ppb)	This work

The selectivity studies of the sensors-encapsulated polymeric membranes were tested by SSM method as shown in Fig. 9a and 9b. Similarly to the sensors in solutions, the result indicated that other metal cations were barely interfered the Hg^{2+} recognition of the sensors. The convenience for using, high selectivity toward Hg^{2+} coupled with high sensitivity Hg^{2+} suggested that the sensors-encapsulated polymeric membranes could be potentially used for on-site Hg^{2+} detection.

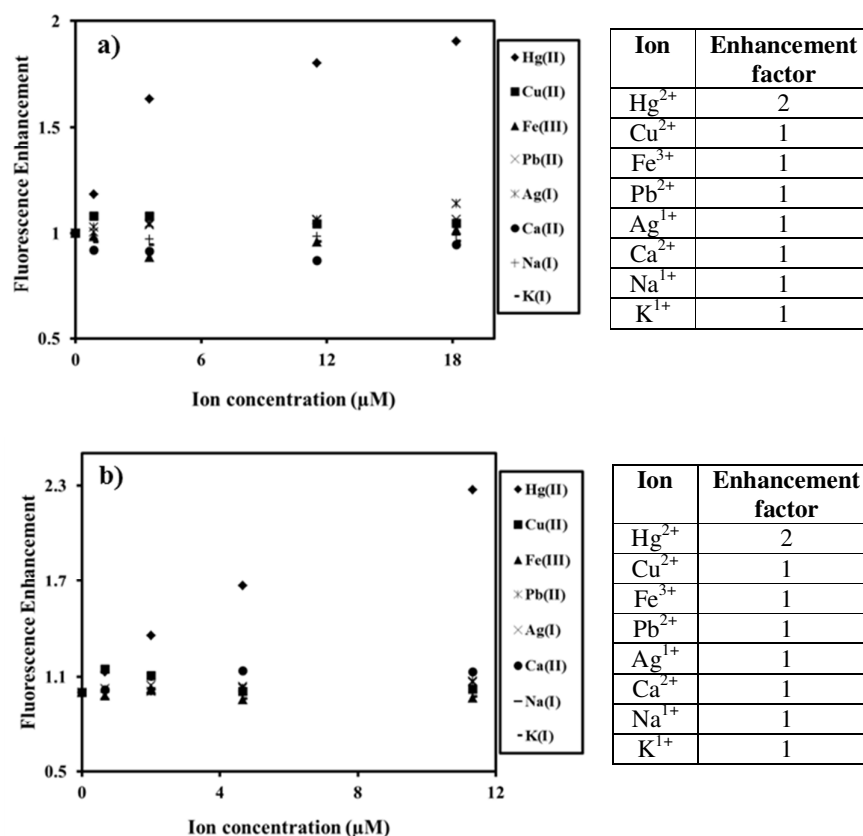


Fig. 9 a) Fluorescence enhancement (658 nm) of polymeric membranes **RBH** as a function of concentrations of various metal ions in 10% v/v MeOH/water ($\lambda_{\text{ex}} = 500$ nm). b) Fluorescence enhancement (665 nm) of polymeric membranes **R6GH** as a function of concentrations of various metal ions in 10% v/v MeOH/water ($\lambda_{\text{ex}} = 500$ nm).

Conclusion

In summary, two Hg²⁺ sensors were designed, synthesized and characterized for utilization of the sensors in solution and polymer film. Sensor **RBH** and **R6GH** were consisted of the rhodamine B moiety and rhodamine 6G moiety, respectively. Encapsulation of the sensors by polymeric membranes (PMMA) provided high selectivity and high sensitivity with sufficient detection limits and convenience for Hg²⁺ detection in environments and various biological systems. Particularly, sensors-encapsulated polymeric membranes **RBH**, showed extremely low detection limit (0.2 ppb) which was 10 times lower than the allowed maximum concentration of Hg²⁺ in the environmental (2 ppb) of US EPA. In aqueous solutions, the sensors exhibited high fluorescence sensitivity in visible wavelength with low detection limits and excellent fluorescence selectivity toward Hg²⁺ which was accompanied by a colorimetric change in the presence of Hg²⁺. Therefore, the developed sensors are suitable for Hg²⁺ detection, especially, the portable sensors-encapsulated polymeric membrane **RBH** which have a potential to be utilized for real time and on-site Hg²⁺ detection.

Acknowledgements

This work was supported by Grant RSA 5680034 from the Thailand Research Fund and Faculty of Science, Silpakorn University, Thailand.

References

- [1] US EPA. *Regulatory impact analysis of the clean air mercury rule*. Final Report. EPA-452/R-05-003. Research Triangle Park, NC: US EPA; 2005.
- [2] V. Celo, D. R. S. Lean, and S. L. Scott, *Sci. Total. Environ.*, 2006, **368**, 126.
- [3] A. Renzoni, F. Zino, and E. Franchi, *Environ. Res.*, 1998, **77**, 68.
- [4] W. F. Fitzgerald, C. H. Lamborg and C. R. Hammerschmidt, *Chem. Rev.*, 2007, **107**, 641.
- [5] Z. C. Zhang, D. Wu, X. F. Guo, X. H. Qian, Z. Lu, Q. Xu, *Chem. Res. Toxicol.*, 2005, **18**, 1814.
- [6] D. W. Boening, *Chemosphere*, 2000, **40**, 1335.
- [7] J. Gutknecht, *J. Membrane. Biol.*, 1981, **61**, 61.
- [8] M. Harada, *Crit. Rev. Toxicol.*, 1995, **25**, 1.
- [9] P. B. Tchounwou, W. K. Ayensu, N. Ninashvili and D. Sutton, *Environ. Toxicol.*, 2003, **18**, 149.
- [10] J. G. Chen, H. W. Chen, X. Z. Jin, and H. T. Chen, *Talanta*, 2009, **77**, 1381.
- [11] L. Ling, Y. Zhao, J. Du, and D. Xiao, *Talanta*, 2012, **91**, 65.
- [12] J. S. Lee, M. S. Han, and C.A. Mirkin, *Angew. Chem. Int. Edit.*, 2007, **46**, 4093.
- [13] T. L. Tan, Y. Q. Zhang, and Y. Chen, *Sens. Actuators B Chem.*, 2011, **156**, 120.
- [14] H. Shoaee, M. Roshdi, N. Khanlarzadeh, and A. Beiraghi, *Spectrochim. Acta Mol. Biomol.*, 2012, **98**, 70.
- [15] P. Mahato, S. Saha, E. Suresh, R. D. Liddo, P. P. Parnigotto, M. T. Conconi, M. K. Kesharwani, B. Ganguly, and A. Das, *Inorg. Chem.*, 2012, **51**, 1769.
- [16] C. Y. Li, F. Xu, Y. F. Li, K. Zhou, and Y. Zhou, *Anal. Chim. Acta.*, 2012, **717**, 122.
- [17] C. Hou, A. M. Urbanec, and H. Cao, *Tet. Lett.*, 2011, **52**, 4903.
- [18] X. -F. Wu, Q. -J. Ma, X. -J. Wei, Y. -M. Hou, and X. Zhu, *Sens. Actuators B Chem.*, 2013, **183**, 565-573.
- [19] N. Wanichacheva, N. Prapawattanapol, V. S. Lee, K. Grudpan, and A. Petsom, *J. Lumin.*, 2013, **134**, 686.
- [20] S. Pandey, A. Azam, S. Pandey, and H. M. Chawla, *Org. Biomol. Chem.*, 2009, **7**, 269.
- [21] N. Wanichacheva, P. Kumsorn, R. Sangsuwan, A. Kamkaew, V. S. Lee, and K. Grudpan, *Tet. Lett.*, 2011, **52**, 6133.
- [22] C. R. Lohani, J. M. Kim, and K. -H. Lee, *Tetrahedron*, 2011, **67**, 4130.
- [23] V. Tharmaraj, and K. Pitchumani, *Anal. Chim. Acta.*, 2012, **751**, 171.
- [24] Y. Cao, L. Ding, W. Hu, L. Wang, and Y. Fang, *Appl. Surf. Sci.*, 2013, **273**, 542.
- [25] X. M. Wang, H. Yan, X. L. Feng, and Y. Chen, *Chinese. Chem. Lett.*, 2010, **21**, 1124.
- [26] L. Chen, B. Zheng, Y. Guo, J. Du, D. Xiao, and L. Bo, *Talanta*, 2013, **117**, 338.
- [27] C. -C. Cheng, Z. -S. Chen, C. -Y. Wu, C. -C. Lin, C. -R. Yang, and Y. -P. Yen, *Sens. Actuators B Chem.*, 2009, **142**, 280.
- [28] J. H. Kim, J. E. Park, M. G. Choi, S. Ahn, and S. -K. Chang, *Dyes. Pigm.*, 2010, **84**, 54.
- [29] X. -F. Yang, Y. Li, and Q. Bai, *Anal. Chim. Acta.*, 2007, **584**, 95.
- [30] H. N. Kim, M. H. Lee, H. J. Kim, J. S. Kim, and J. Yoon, *Chem. Soc. Rev.*, 2008, **37**, 1465.
- [31] M. Beija, C. A. M. Afonso, and J. M. G. Martinho, *Chem. Soc. Rev.*, 2009, **38**, 2410.
- [32] M. H. Lee, J. S. Wu, J. W. Lee, J. H. Jung, and J. S. Kim, *Org. Lett.*, 2007, **9**, 2501.
- [33] J. Y. Kwon, Y. J. Jang, Y. J. Lee, K. M. Kim, M. S. Seo, W. Nam, *J. Am. Chem. Soc.*, 2005, **127**, 10107.
- [34] N. Wanichacheva, K. Setthakarn, N. Prapawattanapol, O. Hanmeng, V. S. Lee, and K. Grudpan, *J. Lumin.*, 2012, **132**, 35.
- [35] N. Wanichacheva, P. Praikaew, T. Suwanich, and K. Sukrat, *Spectrochim. Acta Mol. Biomol.*, 2014, **118**, 908.
- [36] N. Wanichachevaa, O. Hanmeng, S. Kraithong, and K. Sukratc, *J. Photochem. Photobiol. A Chem.*, 2014, **278**, 75.
- [37] Y. Chen, and S. Y. Mu, *J. Lumin.*, 2014, **145**, 760.
- [38] X. Cui, and H. M. Zhang, *J. Lumin.*, 2014, **145**, 364.
- [39] Z. Zhanga, Y. Zheng, W. Hang, X. Yan, and Y. Zhao, *Talanta*, 2011, **85**, 779.
- [40] H. Li, J. Cao, H. Zhu, J. Fan, and X. Peng, *Tet. Lett.*, 2013, **54**, 4357.

- [41] K. N. Kim, M. G. Choi, J. H. Noh, S. Ahn, and S. -K. Chang, *Bull. Korean. Chem. Soc.*, 2008, **29**, 571.
- [42] M. Fischer, J. Georges, *Chem. Phys. Lett.*, 1996, **260**, 115.
- [43] Y. Shiraiishi, S. Sumiya, Y. Kohno, T. Hirai, *J. Org. Chem.*, 2008, **73**, 8571.
- [44] C. Nunez, M. Diniz, A. A. D. Santos, J. L. Capelo, and C. Lodeiro, *Dyes. Pigm.*, 2014, **101**, 156.
- [45] L. Bing, *Sens. Actuators B Chem.*, 2014, **198**, 342.
- [46] Z. Dong, X. Tain, Y. Chen, J. Hou, Y. Guo, J. Sun, and J. Ma, *Dyes. Pigm.*, 2013, **97**, 324.
- [47] W. Huang, D. Wu, G. Wu, and Z. Wang, *Dalton. Trans.*, 2012, **41**, 2625.
- [48] L. Ding, T. Li, Y. Zhong, C. Fan, and J. Huang, *Mater. Sci. Eng. C Mater. Biol. Appl.*, 2014, **35**, 29.
- [49] N. I. Georgiev, R. Bryaskova, R. Tzoneva, I. Ugrinova, C. Detrembleur, S. Miloshev, A. M. Asiri, A. H. Qusti, and V. B. Bojinov, *Bioorgan. Med. Chem.*, 2013, **21**, 6292.
- [50] M. S. Attia, A. M. Othman, A. O. Youssef, and E. E. Raghi, *J. Lumin.*, 2012, **132**, 2049.
- [51] J. Spadavecchia, G. Ciccarella, P. Siciliano, S. Capone, and R., Rella, *Sens. Actuators B Chem.*, 2004, **100**, 88.
- [52] M. J. Frisch, G. W. Trucks, H. B. Schlegel, G. E. Scuseria, M. A. Robb, J. R. Cheeseman, G. Scalmani, V. Barone, B. Mennucci, G. A. Petersson, H. Nakatsuji, M. Caricato, X. Li, H. P. Hratchian, A. F. Izmaylov, J. Bloino, G. Zheng, J. L. Sonnenberg, M. Hada, M. Ehara, K. Toyota, R. Fukuda, J. Hasegawa, M. Ishida, T. Nakajima, Y. Honda, O. Kitao, H. Nakai, T. Vreven, J. A. Montgomery Jr., J. E. Peralta, F. Ogliaro, M. Bearpark, J. J. Heyd, E. Brothers, K. N. Kudin, V. N. Staroverov, T. Keith, R. Kobayashi, J. Normand, K. Raghavachari, A. Rendell, J. C. Burant, S. S. Iyengar, J. Tomasi, M. Cossi, N. Rega, J. M. Millam, M. Klene, J. E. Knox, J. B. Cross, V. Bakken, C. Adamo, J. Jaramillo, R. Gomperts, R. E. Stratmann, O. Yazyev, A. J. Austin, R. Cammi, C. Pomelli, J. W. Ochterski, R. L. Martin, K. Morokuma, V. G. Zakrzewski, G. A. Voth, P. Salvador, J. J. Dannenberg, S. Dapprich, A. D. Daniels, O. Farkas, J. B. Foresman, J. V. Ortiz, J. Cioslowski, D. J. Fox, *GAUSSIAN 09 (Revision B.01)*, Gaussian, Inc., Wallingf.
- [53] M. Shellaiah, Y. C. Rajan, P. Balu, A. Murugan, *New J. Chem.*, 2015, **39**, 2523.
- [54] W. Humphrey, A. Dalke, K. Schulten, *J. Mol. Graph.*, 1996, **14**, 33.
- [55] M. Shortreed, R. Kopelman, M. Kuhn, and B. Hoyland, *Anal. Chem.*, 1996, **68**, 1414.
- [56] J. R. Lakowicz, *Principle of Fluorescence Spectroscopy*, Springer, Singapore, 2006, 248-249.
- [57] Y. Jiao, L. Zhang, P. Zhou, *Talanta*, 2016, **150**, 14.
- [58] Y. Shiraiishi, S. Sumiya, Y., Kohno, and T., Hirai, *J. Org. Chem.*, 2008, **73**, 571.
- [59] M. Li, H. -Y. Lu, R. -L. Liu, J. -D. Chen, and C. -F. Chen, *J. Org. Chem.*, 2012, **77**, 3670.
- [60] P. Mahato, S. Saha, E. Suresh, R. D. Liddo, P. P. Parnigotto, M. T. Conconi, M. K. Kesharwani, B. Ganguly, A. Das, *Inorg. Chem.*, 2012, **51**, 1769–1777.
- [61] M. D. Lumsden, R. E. Wasylshen, K. Eichele, M. Schindler, G. H. Penner, W. P. Power, R. D. Curtist, *J. Am. Chem. SOC.*, 1994, **116**, 1403-1413.
- [62] E. Bakker, P. Buhlmann, and E. Pretsch, *Chem. Rev.*, 1997, **97**, 3083.
- [63] Y. Liu, X. Lv, Y. Zhao, M. Chen, J. Liu, P. Wang, and W. Guo, *Dyes. Pigm.*, 2012, **92**, 909.
- [64] G. He, X. Zhang, C. He, X. Zhao, and C. Duan, *Tetrahedron*, 2010, **66**, 9762.
- [65] S. M. Park, M. H. Kim, J. I. Choe, K. T. No, and S. -K. Chang, *J. Org. Chem.*, 2007, **72**, 3550.
- [66] K. -C. Song, M. H. Kim, H. J. Kim, and S. -K. Chang, *Tet. Lett.*, 2007, **48**, 7464.
- [67] J. Tan, X. -P., Yan, *Talanta*, 2008, **76**, 9.
- [68] K. N. N. Unni, S. Dabos-Seignon, J.-M. Nunzi, *J. Mater. Sci.*, 2006, **41**, 1865.
- [69] M. Wang, J. Wen, Z. Qin, H. Wang, *Dyes. Pigment.*, 2015, **120**, 208-212.
- [70] C. Arivazhagan, R. Borthakur, S. Ghosh, *Organometallics*, 2015, **34**, 1147-1155.
- [71] N. R. Chereddy, P. Nagaraju, M. V. N. Raju, K. Saranraj, S. Thennarasu, V. J. Rao, *Dyes. Pigments*. 2015, **112**, 201-209.
- [72] Y. Fanga, Y. Zhoua, J. -Y. Lia, Q.- Q. Ruia, C. Yaoa, *Sens. Actuators B Chem.*, 2015, **215**, 350-359.

- [73] D. Wu, W. Huang, Z. Lin, C. Duan, C. He, S. Wu, D. Wang, *Inorg. Chem.*, 2008, **47**, 7190-7201.